VERSITA

Chemical Papers 64 (3) 318–328 (2010)
DOI: 10.2478/s11696-010-0003-0

ORIGINAL PAPER

# Synthesis, DNA binding, and antimicrobial studies of novel metal complexes containing a pyrazolone derivative Schiff base

[a]Natarajan Raman*, [a]Ramaraj Jeyamurugan, [a]Mariyyappan Subbulakshmi, [a]Raja Boominathan, [b]Chithu Ramakrishnan Yuvarajan

[a] *Research Department of Chemistry, VHNSN College, Virudhunagar-626 001, India*

[b] *Department of Chemistry, Sourashtra College, Madurai-625 004, India*

Received 21 June 2009; Revised 31 August 2009; Accepted 4 September 2009

A novel series of Co(II), Ni(II), Cu(II), Zn(II), and VO(IV) complexes has been synthesized from the Schiff base derived from 4-[(3,4-dimethoxybenzylidene)amino]-1,5-dimethyl-2-phenyl-1,2-dihydropyrazol-3-one and 1,2-diaminobenzene. Structural features were determined by analytical and spectral techniques. Binding of synthesized complexes with calf thymus DNA (CT DNA) was studied by spectroscopic methods and viscosity measurements. Experimental results indicate that the complexes are able to form adducts with DNA and to distort the double helix by changing the base stacking. Lower DNA affinity of the VO(IV) complex is caused by the change of coordination geometry by the vanadyl ion resulting in a somewhat unfavorable configuration for the DNA binding. Oxidative DNA cleavage activities of the complexes were studied with supercoiled (SC) pUC19 DNA using gel electrophoresis; the mechanism studies revealed that the hydroxyl radical is likely to be the reactive species responsible for the cleavage of pUC19 DNA by the synthesized complexes. The in vitro antimicrobial screening effects of the investigated compounds were monitored by the disc diffusion method. The synthesized Schiff base complexes exhibit higher antimicrobial activity than the respective free Schiff base.


**Keywords:** pyrazolone, Schiff base, complexes, DNA binding, oxidative cleavage, antimicrobial

## Introduction

Coordination metal complexes have been gaining increasing importance in recent years; particularly in the design of repository, slow release long acting drugs in nutrition and in the study of metabolism (Terenzi et al., 2009). Recent years have witnessed a great deal of interest in the synthesis and characterization of transition metal complexes of pyrazolone derivatives. Among these derivatives, 4-aminoantipyrine is a remarkable reagent due to its importance in biological, pharmacological, clinical, and analytical applications. Earlier works reported that some drugs show increased activity when administrated as metal chelates rather than as organic compounds. A number of metal chelates are of current interest due to their important applications in nucleic acid chemistry as DNA probes of DNA structure in solutions, reagents for the mediation of strand scission of duplex DNA under physicochemical conditions, and as chemotherapeutic agents and in the genomic research (Raman et al., 2008; Lu et al., 2002).

The interaction between DNA and transition metal complexes is an important fundamental issue in life sciences. These complexes can bind to DNA in noncovalent modes such as electrostatic, intercalative, and groove binding. The above applications require that the complex binds to DNA through an intercalative mode wherein the planar aromatic heterocyclic group is inserted and stacked between the base pairs of DNA (Raman & Jeyamurugan, 2009), which is related to the in vivo replication and transcription of DNA, mu-

*Corresponding author, e-mail: drn_raman@yahoo.co.in

tation of genes, variations of species in their character, and to the action mechanism of some synthetic chemical nucleases (Lu et al., 2002). Moreover, oxidative cleavage of DNA on irradiation with visible light has gained considerable interest due to its potential application in photodynamic therapy of cancer (Mitsopoulou et al., 2008). Considering all these facts, DNA binding and oxidative cleavage activity of pyrazolone derivative transition metal complexes, with interesting physical and spectroscopic properties, have become our main interest.

## Experimental

All reagents and chemicals were procured from Merck (Darmstadt, Germany). Solvents used for electrochemical and spectroscopic studies were purified by standard procedures (Perrin et al., 1980). DNA was purchased from Bangalore Genei (India). Agarose (molecular biology grade) and ethidium bromide (EB) were obtained from Sigma–Aldrich (St. Louis, Missouri, USA). Tris(hydroxymethyl)aminomethane hydrochloride (Tris–HCl) buffer solution was prepared using deionized, sonicated, triply distilled water.

Elemental analyses of the complexes were carried out on a CHN analyzer Carlo Erba 1108, Heraeus. Infrared spectra (4000–400 $cm^{-1}$, KBr discs) of the samples were recorded on a Perkin–Elmer 783 series FTIR spectrophotometer. Electronic absorption spectra (in DMF at room temperature) in the range of 200–1100 nm were obtained on a Shimadzu UV-1601 spectrophotometer. $^1H$ NMR spectra (300 MHz) of the ligand and its zinc complex were recorded on a Bruker Avance DRX 300 FT-NMR spectrometer using $CDCl_3$ and DMSO-$d_6$ as solvents, respectively. Fast atom bombardment mass spectra (FAB-MS) were obtained in a 3-nitrobenzyl alcohol matrix using a VGZAB-HS spectrometer. X-band EPR spectra of the complexes were recorded at room temperature and at −196 °C, respectively, using tetracyanoethylene (TCNE) as the g-marker. Molar conductivity of $10^{-3}$ M solutions of the complexes in DMF were measured at room temperature with a Deepvision Model-601 digital direct reading deluxe conductivity meter. Magnetic susceptibility measurements were carried out by employing the Guoy method at room temperature on a powdered sample of the complex. $CuSO_4 \cdot 5H_2O$ was used as the calibrant. Metal contents of the complexes were determined according to a literature method (Angelici, 1969). Chloride ion was determined gravimetrically as silver chloride. Purity of the ligand and its complexes was evaluated by column chromatography and thin layer chromatography.

All experiments involving the interaction of synthesized complexes with CT DNA were carried out in a Tris–HCl buffer (50 mM Tris–HCl, pH = 7.2) containing 5 % of ethanol at room temperature. Solutions of CT DNA in the above buffer gave a ratio of UV absorbance at 260 nm and 280 nm, $A_{260}/A_{280}$ of 1.87, indicating that the CT DNA was sufficiently free from protein (Marmur, 1961). The CT DNA concentration per nucleotide was determined by absorption spectroscopy at 260 nm using the molar absorption coefficient $\varepsilon_{260}$ (6600 $M^{-1}$ $cm^{-1}$) (Reichmann et al., 1954).

Absorption titration experiments were performed by maintaining constant metal complex concentration of 25 μM while varying the concentration of CT DNA within 0 μM to 400 μM. While measuring the absorption spectra, equal quantity of CT DNA was added to both the complex solution and the reference solution to eliminate the absorbance of CT DNA itself. From the absorption data, the intrinsic binding constant $K_b$ was determined from a plot of $[DNA]/(\varepsilon_a - \varepsilon_f)$ versus [DNA] using the equation

$$[DNA]/(\varepsilon_a - \varepsilon_f) = [DNA]/(\varepsilon_b - \varepsilon_f) + [K_b(\varepsilon_b - \varepsilon_f)]^{-1} \quad (1)$$

where [DNA] is the concentration of CT DNA in base pairs. The apparent absorption coefficients $\varepsilon_a$, $\varepsilon_f$, and $\varepsilon_b$ correspond to $A_{obsd}/[M]$ (where M = metal), to the extinction coefficient for the free M(II) complex and to the extinction coefficient for the M(II) complex in the fully bound form, respectively. $K_b$ is given by the ratio of slope to the intercept.

Cyclic voltammetric and differential pulse voltammogram studies were performed on a CHI 620C electrochemical analyzer with a three electrode system of glassy carbon (GC) as the working electrode, a platinum wire as the auxiliary electrode and Ag/AgCl as the reference electrode. All voltammetric experiments were carried out in single-compartment cells of the volume of 5–15 mL. Solutions were deoxygenated by purging with $N_2$ prior to the measurements. Increasing amounts of CT DNA were added directly into the cell containing the solution ($2.5 \times 10^{-3}$ M, 5 mM Tris-HCl/50 mM NaCl buffer, pH = 7.1). The concentration of CT DNA ranged from 0 μM to 400 μM. The solution in the cuvette was thoroughly mixed before each scan. All experiments were carried out at room temperature.

Viscosity experiments were carried out on an Ostwald viscometer, immersed in a thermostated waterbath maintained at the constant temperature of (30.0 ± 0.1) °C. CT DNA samples of approximately 0.5 mM were prepared by sonication in order to minimize the complexities arising from CT DNA flexibility (Sathyanarayana et al., 1993). Flow time was measured with a digital stopwatch three times for each sample and the average flow time was calculated. Data were presented as $(\eta/\eta^\circ)^{1/3}$ versus the concentration of the M(II) complexes, where $\eta$ is the viscosity of the CT DNA solution in the presence of the complex, and $\eta^\circ$ is the viscosity of the CT DNA solution in the absence of the complex. Viscosity values were calculated

after correcting the flow time of buffer alone ($t_0$), $\eta = (t - t_0)/t_0$.

Extent of the cleavage of super coiled (SC) pUC19 DNA (33.3 μM, 0.2 μg) to its nicked circular (NC) form was determined by agarose gel electrophoresis in a 50 mM Tris–HCl buffer (pH = 7.2) containing 50 mM NaCl. The gel electrophoresis experiments were performed by incubation of 30 μM pUC19 DNA, 50 μM of each complex and 50 μM 3-mercaptopropionic acid (MPA) in the Tris–HCl buffer (pH = 7.2) at 37 °C for 2 h. After the incubation, the samples were electrophorezed for 2 h at 100 V on a 0.8 % agarose gel using the Tris–acetic acid–EDTA buffer (pH = 7.2). The gel was then stained using 1 μM ethidium bromide (EB) and photographed under ultraviolet light at 360 nm.

The synthesized ligand and its complexes were tested for their in vitro antimicrobial activity against the Gram-positive bacteria *Staphylococcus aureus*, *Bacillus subtilis*, the Gram-negative bacteria *Escherichia coli*, *Salmonella typhi* by the disc diffusion method using agar nutrient as the medium, and against the fungi *Aspergillus niger*, *Aspergillus flavus*, *Candida albicans*, and *Rhizoctonia bataicola* by the well known diffusion method using potato dextrose agar as the medium. The stock solution ($10^{-2}$ M) was prepared by dissolving the compounds in DMSO, the solutions were then serially diluted in order to find the minimum inhibitory concentration (MIC) values (Kannan, 1996). Streptomycin and nystatin were used as control drugs.

The Schiff base ligand and its Co(II), Ni(II), Cu(II), Zn(II), and VO(IV) complexes were prepared as follows: an ethanolic solution (20 mL) of 4-aminoantipyrine (2.03 g, 0.01 mol) was added to an ethanolic solution (20 mL) of 3,4-dimethoxybenzaldehyde (1.06 g, 0.01 mol). On stirring, the solid product separated. It was filtered, recrystallized from ethanol and added (2.9 g, 0.01 mol) to an ethanolic solution (20 mL) of 1,2-diaminobenzene (0.54 g, 0.005 mol). After an addition of $K_2CO_3$, the mixture was heated under reflux for about 30 h. Separated solid product was filtered and recrystallized from ethanol to give the corresponding Schiff base (ligand L) (Fig. 1). This ligand (0.675 g, 0.001 mol), dissolved in hot ethanol (50 mL), was added to a hot ethanolic solution (25 mL) of metal salts (0.17 g, 0.001 mol) and heated under reflux for approximately 4 h. The resulting solution was reduced on a water bath to one third. The pasty mass obtained was treated with ether and the solid obtained was filtered and washed with ethanol and dried in vacuo.

## Results and discussion

The synthesized ligand and its Co(II), Ni(II), Cu(II), Zn(II), and VO(IV) complexes were found to be air-stable. The ligand is soluble in common organic solvents but the complexes are soluble only in DMF and DMSO. The ligand and its complexes were characterized by analytical and spectral techniques. Physical characterization, microanalytical, and molar conductivity data of the complexes are given in Table 1. Analytical data of the complexes correspond well with the general formula [ML]X (where X = $Cl_2$ or $SO_4^{2-}$) except for the cobalt complex whose formula is $MLCl_2$. Monomeric nature of the complexes was confirmed from their magnetic susceptibility data. The observed high molar conductivity of the complexes in DMF at room temperature is consistent with the electrolytic nature of the complexes due to counter ions (chloride/sulfate) in the structure of all the complexes except for the cobalt complex which has low molar conductivity indicating its non-electrolytic nature. Elemental analysis results for the metal complexes agree with the calculated values showing that the complexes have the metal/ligand ratio of 1 : 1. Presence of the chloride ion is evident from the Volhard's test and that of the sulfate ion from the $BaCl_2$ test.

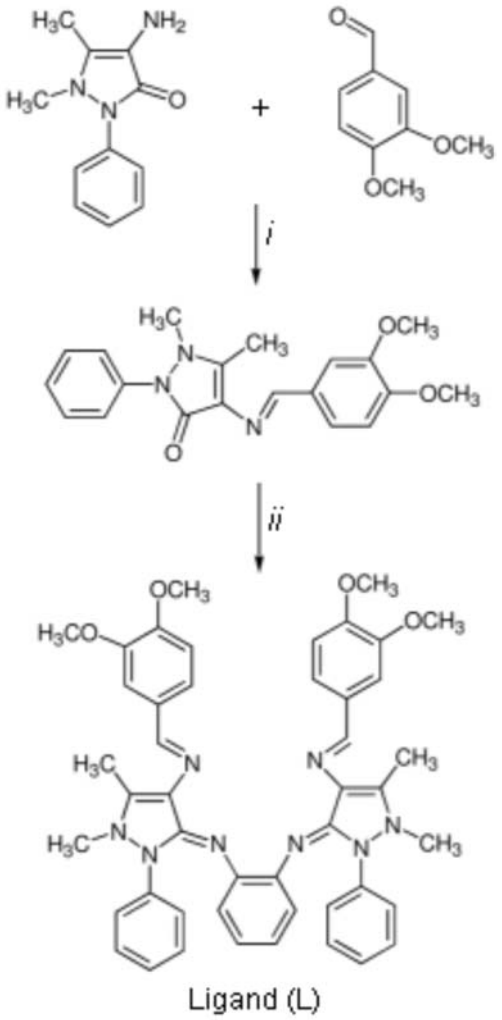


**Fig. 1.** Synthesis of ligand (L). Reaction conditions: *i*) stirring at room temperature; *ii*) 1,2-diaminobenzene, $K_2CO_3$, reflux, 30 h.

**Table 1.** Physical characterization, analytical, molar conductance, and magnetic susceptibility data for the ligand and its complexes

| Compound | Color | Formula | Yield (%) | $w_i$(calc.) (mass %) $w_i$(found) (mass %) | | | | Molar conductivity (S cm$^2$ mol$^{-1}$) |
|---|---|---|---|---|---|---|---|---|
| | | | | M | C | H | N | |
| Ligand | yellow | $C_{46}H_{46}N_8O_4$ | 72 | – | 71.3 | 5.9 | 14.5 | – |
| | | | | | 71.0 | 5.7 | 14.1 | |
| $[CuL]Cl_2$ | black | $[CuC_{46}H_{46}N_8O_4]Cl_2$ | 61 | 7.8 | 60.8 | 5.1 | 7.0 | 129 |
| | | | | 7.6 | 60.7 | 5.1 | 6.8 | |
| $[NiL]Cl_2$ | light green | $[NiC_{46}H_{46}N_8O_4]Cl_2$ | 48 | 6.5 | 61.1 | 5.1 | 12.4 | 146 |
| | | | | 6.3 | 60.8 | 5.1 | 12.2 | |
| $[ZnL]Cl_2$ | grey | $[ZnC_{46}H_{46}N_8O_4]Cl_2$ | 36 | 7.2 | 60.6 | 5.1 | 12.3 | 137 |
| | | | | 7.0 | 60.3 | 5.1 | 12.1 | |
| $[VOL]SO_4$ | green | $[VC_{46}H_{46}N_8O_5]SO_4$ | 54 | 5.4 | 58.9 | 4.9 | 12.0 | 128 |
| | | | | 5.1 | 58.7 | 5.1 | 11.8 | |
| $[CoLCl_2]$ | brown | $[CoC_{46}H_{46}N_8O_4Cl_2]$ | 49 | 6.5 | 61.1 | 5.1 | 12.4 | 2.2 |
| | | | | 6.2 | 60.7 | 5.1 | 12.2 | |

**Table 2.** Electronic absorption spectral data of the compounds

| Compound | Absorption (cm$^{-1}$) | Band assignment | $\mu_{eff}$ (B.M.) | Geometry |
|---|---|---|---|---|
| $[CuL]Cl_2$ | 21186 | $^2B_{1g} \rightarrow {}^2A_{1g}$ | 1.69 | Square-planar |
| $[CoLCl_2]$ | 12108 | $^4T_{1g}$ (F) $\rightarrow {}^4T_{2g}$ (F) | 4.87 | Octahedral |
| | 14254 | $^4T_{1g}$ (F) $\rightarrow {}^4A_{2g}$ (F) | | |
| | 19586 | $^4T_{1g}$ (F) $\rightarrow {}^4T_{2g}$ (P) | | |
| $[NiL]Cl_2$ | 22658 | $^1A_{1g} \rightarrow {}^1A_{2g}$ | – | Square-planar |
| | 17605 | $^1A_{1g} \rightarrow {}^1B_{1g}$ | | |
| $[VO]SO_4$ | 19267 | $^2B_2 \rightarrow {}^2A_1$ | 1.74 | Square-pyramidal |
| | 13879 | $^2B_2 \rightarrow {}^2E$ | | |

FAB-MS spectra of the synthesized ligand and its complexes were recorded and the obtained molecular ion peaks confirm the proposed formulae. Mass spectrum of the ligand shows a molecular ion peak ($M^+$) at $m/z$ 775 corresponding to $[C_{46}H_{46}N_8O_4]^+$ ion. Its copper complex shows the $M^+$ peak at $m/z$ 910 and another important peak appeared at $m/z$ 838, which suggests the loss of two chloride ions. These data confirm the stoichiometry of the $[CuL]Cl_2$ type. This is further supported by the mass spectra of all the complexes. The observed peaks are in good agreement with their empirical formulae as indicated by the microanalytical data. Thus, the mass spectral data support the conclusions drawn from the analytical and high molar conductivity values. The cobalt complex shows the $M^+$ peak at $m/z$ 905 and the absence of the peak at $m/z$ 834, which confirms the stoichiometry of the $[CoLCl_2]$ type which is further supported by the analytical and low molar conductivity values.

Spectrum of the free Schiff base ligand shows a band of the C═N group in the region of 1635 cm$^{-1}$, which is shifted to lower frequencies in the spectra of all complexes (1615–1605 cm$^{-1}$) indicating the involvement of —C═N nitrogen in coordination to the metal ion (Priya et al., 2009). Coordination of the Schiff base to the metal through the nitrogen atom is expected to reduce the electron density in the azomethine link and to lower the $\nu$(C═N) vibration. All complexes show bands in the 1090–1100 cm$^{-1}$ and 700–750 cm$^{-1}$ regions which can be assigned to the phenyl ring vibrations. Assignment of the proposed coordination sites is further supported by the appearance of medium bands at 450–500 cm$^{-1}$ which can be attributed to the $\nu$(M—N) vibrations (Firdaus et al., 2009). The vanadyl complex shows a band at 963 cm$^{-1}$ assigned to the $\nu$(V═O) vibration (Raman et al., 2009).

Electronic spectra serve as a tool to distinguish between the square-planar, octahedral, and tetrahedral geometries of the complexes. The absorption regions, assignment and the proposed geometry of the complexes are given in Table 2. The copper complex is magnetically normal with a magnetic moment of 1.69 B.M. Electronic absorption of the copper complex in the DMF solution shows a *d*–*d* transition at about 21186 cm$^{-1}$ which can be assigned as the $^2B_{1g} \rightarrow {}^2A_{1g}$ transition, revealing that the Cu(II) complex exists in the square-planar geometry (Lever, 1968).

Electronic spectrum of the cobalt complex exhibits a broad weak band in the regions of 12108 cm$^{-1}$,

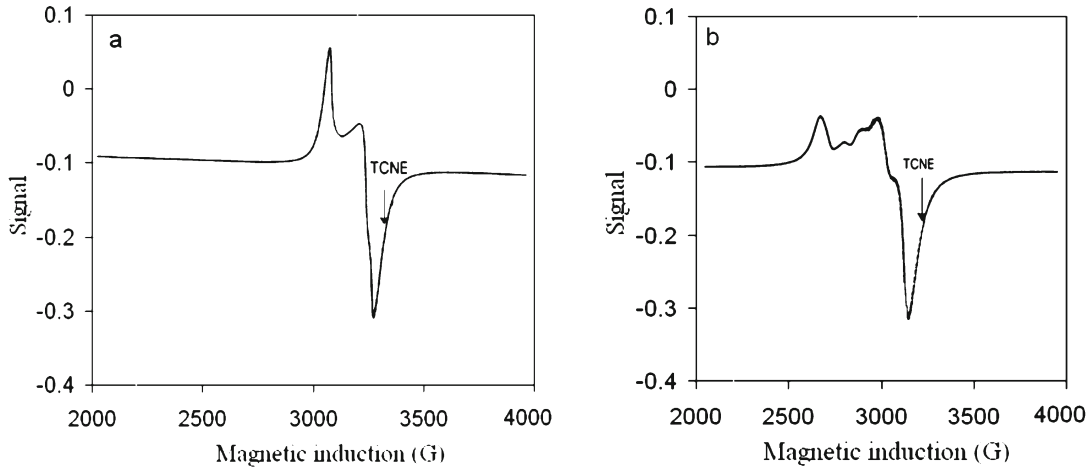


**Fig. 2.** EPR spectra of the copper complex at room temperature (a) and at −196 °C (b).

14254 $cm^{-1}$, and 19586 $cm^{-1}$, suggesting an octahedral geometry. The room temperature magnetic moment (4.87 B.M.) determined for the Co(II) complex is higher than the spin-only magnetic moment ($\mu_{eff}$ = 3.87 B.M.) of three unpaired electrons, which is due to the spin-orbit coupling contribution and indicates high spin nature (Sharada & Syamal, 1992). The observed zero magnetic moment confirms the square-planar environment of the nickel complex in conformity considering the fact that all known square-planar complexes of nickel are diamagnetic. The Ni(II) complex shows two *d*–*d* transitions at about 22658 $cm^{-1}$ ($^1A_{1g} \rightarrow {}^1A_{2g}$) and 17605 $cm^{-1}$ ($^1A_{1g} \rightarrow {}^1B_{1g}$) which reveal that the nickel complex exists in the square-planar environment (Lever, 1968). Electronic absorption spectrum of the vanadyl complex exhibits two *d*–*d* bands at 19267 $cm^{-1}$ and 13879 $cm^{-1}$ which are assigned to the $^2B_2 \rightarrow {}^2A_1$ and $^2B_2 \rightarrow {}^2E$ transitions, respectively. A square-pyramidal geometry is proposed for this system because it shows a band at 13879 $cm^{-1}$ ($^2B_2 \rightarrow {}^2E$) (Sharada & Syamal, 1992), which was further confirmed by its EPR spectral data.

$^1$H NMR spectra of the ligand show the following signals: $\delta$ = 7.0–7.5 (m, phenyl), $\delta$ = 3.0 ($NCH_3$), $\delta$ = 7.9 (CH═N), $\delta$ = 3.8 ($OCH_3$), $\delta$ = 2.2 (C—$CH_3$). The azomethine proton (CH═N) signal in the spectrum of the zinc complex is shifted downfield compared to the free ligand, suggesting the deshielding of the azomethine group due to its coordination to the metal ion. There is no appreciable change in the other signals of the complex.

X-band EPR spectrum of the complex at room temperature (Fig. 2a) shows an intense absorption band in the high field region, which is caused by the tumbling motion of the molecules. However, this complex in the frozen state (−196 °C) shows four well resolved peaks (Fig. 2b) with low intensities in the low field region and one intense peak in the high field region. The value of magnetic susceptibility reveals that the copper complex has a magnetic moment of 1.69 B.M. which corresponds to one unpaired electron indicating that the complex is mononuclear. This fact is also evident from the absence of a half field signal observed in the spectrum at 1600 G due to the $m_s = \pm 2$ transitions ruling out any Cu–Cu interaction (Raman et al., 2009).

In square-planar complexes, the unpaired electron lies in the $d_{x^2-y^2}$ orbitals giving $^2B_{1g}$ as the ground state with $g_\parallel > g_\perp > 2$, while the unpaired electron lies in the $d_z^2$ orbital giving $^2A_1$g as the ground state with $g_\perp > g_\parallel > 2$. From the observed values ($A_\parallel$ = 147 > $A_\perp$ = 58; $g_\parallel$ = 2.29 > $g_\perp$ = 2.06 > 2.0023) it is clear that the EPR parameters of the complex coincide well with the related systems, which suggests that the complex has square-planar geometry and the system is axially symmetrical (Ray & Kauffman, 1990). This is also supported by the fact that the unpaired electron lies predominantly in the $d_{x^2-y^2}$ orbital. In the axial spectra, the g-values are related with the exchange interaction coupling constant ($G$) by the expression: $G = g_\parallel - 2.0023/g_\perp - 2.0023$. According to Dudley and Hathaway (1970), if the $G$ value is larger than four, the exchange interaction is negligible because the local tetragonal axes are parallel or slightly misaligned. If the value of $G$ is less than four, the exchange interaction is considerable and the local tetragonal axes are misaligned. For the presented copper complex, the $G$ value is 4.9 suggesting that the local tetragonal axes are parallel or slightly misaligned and consistent with a $d_{x^2-y^2}$ ground state.

Covalent bonding parameters for the Cu(II) ion in various ligand field environments are usually determined. The in-plane $\sigma$-bonding covalency parameter $\alpha^2$ is related to $A_\parallel$, $g_\parallel$ and $g_\perp$ according to the following equation

$$\alpha^2 = (A_\parallel/P) + (g_\parallel - 2.0023) + \\ + 3/7(g_\perp - 2.0023) + 0.04 \qquad (2)$$

If the $\alpha^2$ value is 0.5, it indicates complete covalent

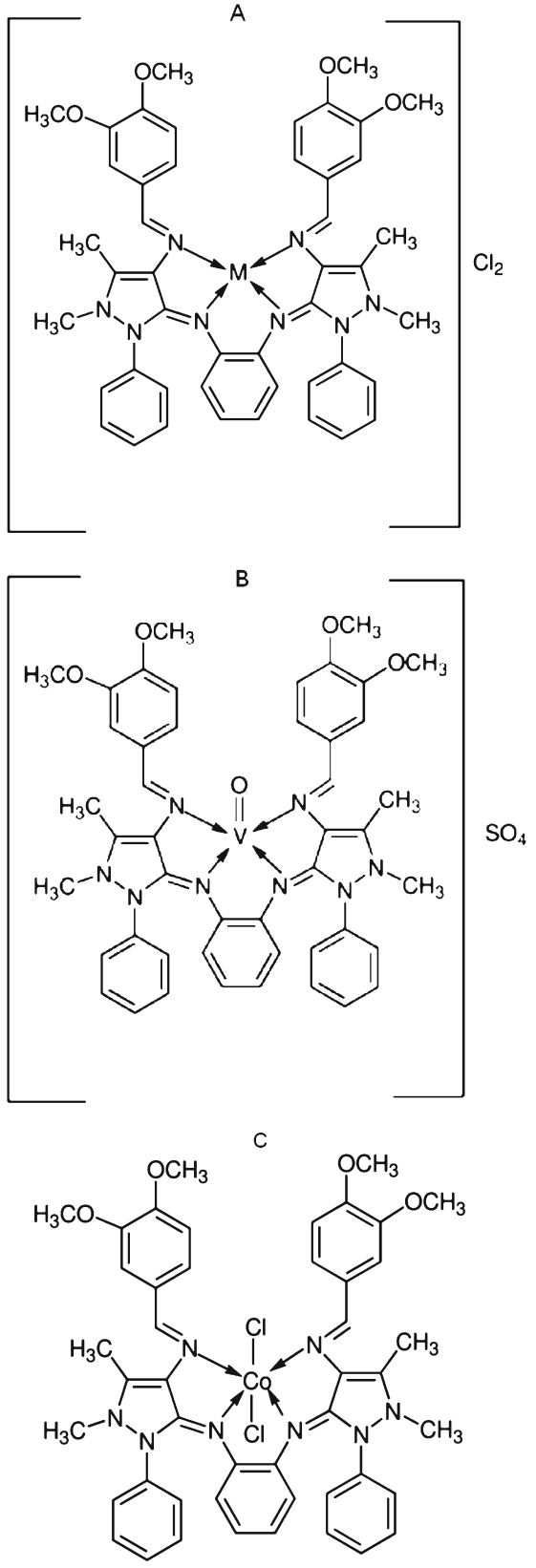


**Fig. 3.** Structure of complexes: $[ML]Cl_2$ general type (A), $[VOL]SO_4$ (B), $[CoLCl_2]$ (C).

bonding, while the value of 1.0 suggests complete ionic bonding. The observed value of $\alpha^2$ (0.7) indicates that the complexes have some covalent character. The out-of-plane $\pi$ bonding ($\gamma^2$) and in the plane $\pi$-bonding ($\beta^2$) parameters are calculated from the following expressions

$$\beta^2 = (g_{\parallel} - 2.0023)E/(-8\lambda\alpha^2) \quad (3)$$

$$\gamma^2 = (g_{\perp} - 2.0023)E/(-2\lambda\alpha^2) \quad (4)$$

In these equations $\lambda = -828$ cm$^{-1}$ for the free metal ion and $E = 17271$ cm$^{-1}$. The observed $\beta^2$ (1.29) and $\alpha^2$ (0.7) values indicate that there is an interaction in the out-of-plane $\pi$-bonding, whereas the in-plane $\pi$-bonding is completely covalent. This is also confirmed by the orbital reduction factors (Dodwad et al., 1989) estimated using the relations: $K_{\parallel} = (g_{\parallel} - 2.0023)(\Delta E/-8\lambda)$ and $K_{\perp} = (g_{\perp} - 2.0023)(\Delta E/-8\lambda)$. Significant information on the nature of bonding in the Cu(II) complex can be derived from the relative magnitudes of $K_{\parallel}$ and $K_{\perp}$. In case of pure $\sigma$-bonding $K_{\parallel} \approx K_{\perp} = 0.77$, whereas $K_{\parallel} < K_{\perp}$ implies a considerable in-plane $\pi$-bonding, while for the out-of-plane $\pi$-bonding $K_{\parallel} > K_{\perp}$ . For the presented complex, the observed order is $K_{||}$ (0.96) > $K_{\parallel}$ (0.42) implying a greater contribution from the out-of-plane $\pi$-bonding than from the in-plane $\pi$-bonding in the metal ligand $\pi$-bonding. Thus, the EPR study of the copper complex provided supporting evidence for the optical results.

EPR spectrum of the vanadyl complex at room temperature is a typical eight-line pattern, which shows that a single vanadium atom is present in the molecule, i.e., it is a monomer. In the frozen solid state, the spectrum shows two types of resonances: one set is caused by the parallel features and the other by the perpendicular features which show an axially symmetric anisotropy with a well resolved 16-lines hyperfine splitting characteristic of an interaction between the electron and the vanadium nuclear spin. The observed anisotropic parameter values ($g_{\parallel} = 1.92$, $g_{\perp} = 1.98$, $A_{\parallel} = 174$, and $A_{\perp} = 75$) indicate that the unpaired electron is present in the $d_{xy}$ orbital with the square-pyramidal geometry around the VO(IV) chelate (Dodwad et al., 1989; Yen, 1969). Based on the spectral data, structures of the synthesized complexes are given in Figs. 3A–3C.

Absorption spectrum of the copper complex in the absence and in the presence of CT DNA is shown in Fig. 4. With increasing CT DNA concentration, for copper complex, the hypochromism in the band at 410.5 nm reaches 10.2 % with a blue shift of 4.5 nm. These spectral characteristics obviously suggest that the copper complex interacts with DNA most likely through a mode that involves a stacking interaction between the aromatic chromophore and the base pairs of DNA. After intercalating the base pairs of DNA, the $\pi^*$ orbital of the intercalated ligand can couple with the $\pi$ orbital of the base pairs thus de-

**Table 3.** Absorption spectral properties of synthesized complexes with CT DNA

| Complexes | $\lambda_{max}$ (nm) | | $\Delta\lambda$ (nm) | H (%) | $K_b \cdot 10^4$ (dm$^3$ mol$^{-1}$) |
|---|---|---|---|---|---|
| | Free | Bound | | | |
| $[CuL]Cl_2$ | 410.5 | 413.0 | 2.5 | 10.2 | 4.4 |
| $[ZnL]Cl_2$ | 402.0 | 404.0 | 2.0 | 8.2 | 3.0 |
| $[CoLCl_2]$ | 395.0 | 392.6 | 2.4 | 9.8 | 3.6 |
| $[NiL]Cl_2$ | 405.0 | 403.3 | 2.3 | 6.9 | 2.9 |
| $[VOL]Cl_2$ | 404.0 | 403.5 | 0.5 | 0.6 | – |

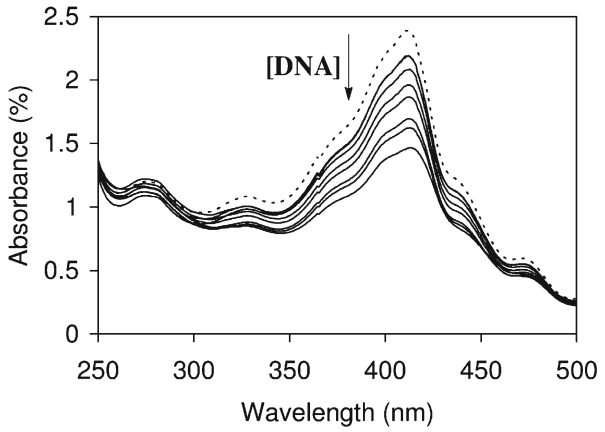


**Fig. 4.** Changes in the electronic absorption spectrum of $[CuL]Cl_2$ in 50 mM Tris-HCl buffer (pH 7.2, 25 °C) in the absence (dashed line) and in the presence (solid lines) of CT DNA.

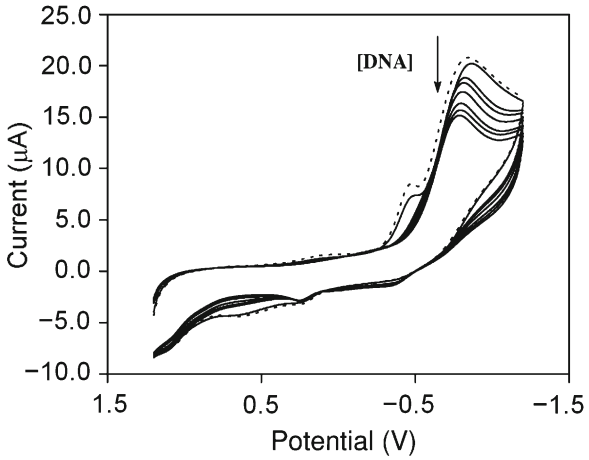


**Fig. 5.** Cyclic voltammogram of $[CuL]Cl_2$ in the absence (dashed line) and in the presence (solid lines) of different concentrations of DNA.

creasing the $\pi$–$\pi^*$ transition energy and resulting in bathochromism. On the other hand, the coupling $\pi$ orbital is partially filled by electrons thus decreasing the transition probabilities and concomitantly resulting in hypochromism. The intrinsic binding constant $K_b$ can be obtained from the ratio of the slope to the intercept of the plots of [DNA]/($\varepsilon_a - \varepsilon_f$) vs. [DNA].

To compare quantitatively the affinity of the synthesized complexes towards DNA, the intrinsic binding constants $K_b$ of the synthesized complexes to CT DNA are shown in Table 3. From these results, very weak hypochromism and no significant spectral shift were found after the vanadyl complex was mixed with DNA which indicates that the vanadyl complex forms weaker adduct to CT DNA than the other complexes. The lower DNA affinity of the vanadyl complex might be explained by the change of the coordination geometry by vanadyl ion chelation which may result in a somewhat unfavorable configuration for the DNA binding.

Cyclic and differential pulse voltammetric techniques are extremely useful in probing the nature and mode of DNA binding of metal complexes. Typical cyclic voltammogram of copper complex in the absence and in the presence of varying amount of [DNA] is shown in Fig. 5. In the absence of CT DNA, the first redox couple cathodic peak appears at −0.251 V for Cu(II) → Cu(I) ($Ep_a$ = −0.893 V, $Ep_c$ = −0.727 V, $\Delta Ep$ = 0.166 V, and $E_{1/2}$ = 0.81 V). The $ip_c/ip_a$ ratio of this redox couple is less than one. This indicates that reaction of the complex on the glassy carbon electrode surface is a quasi-reversible redox process. Incremental addition of CT DNA to the complex causes a negative shift in $E_{1/2}$ and an increase in $\Delta Ep$. The $ip_c/ip_a$ values also decrease in the presence of DNA. The decrease of the anodic and cathodic peak currents of the complex in the presence of DNA is due to the decrease in the apparent diffusion coefficient of the Cu(II) complex upon its complexation with the DNA macromolecule. The second redox couple, Cu(III) → Cu(II), shows no significant change in the potential and current intensity in the presence of CT DNA. These results show that the Cu(II) complex stabilizes the duplex (GC pairs) by intercalation. Electrochemical parameters of the synthesized Co(II), Ni(II), Cu(II), and VO(IV) complexes are shown in Table 4. These results indicate that the synthesized complexes may stabilize the duplex DNA. In the absence of CT DNA, the redox couple anodic peak appears at −0.286 V. Incremental addition of DNA to the Zn(II) complexes shows a decrease in the current intensity and a negative shift of the oxidation peak

**Table 4.** Electrochemical parameters of the interaction of DNA with Co(II), Ni(II), and Cu(II) complexes

| Complexes | Redox couple | $E_{1/2}$ (V) | | $\Delta E$p (V) | | $K_{[red]}/K_{[oxd]}$ | $I_{pc}/I_{pa}$ |
|---|---|---|---|---|---|---|---|
| | | Free | Bound | Free | Bound | | |
| $[CoLCl_2]$ | Co(III)/Co(II) | 0.438 | 0.407 | 0.348 | 0.382 | 1.34 | 0.82 |
| $[NiL]Cl_2$ | Ni(II)/Ni(I) | −0.325 | −0.312 | 0.315 | 0.332 | 0.75 | 0.76 |
| $[CuL]Cl_2$ | Cu(II)/Cu(I) | 0.810 | 0.795 | 0.166 | 0.194 | 0.84 | 0.91 |

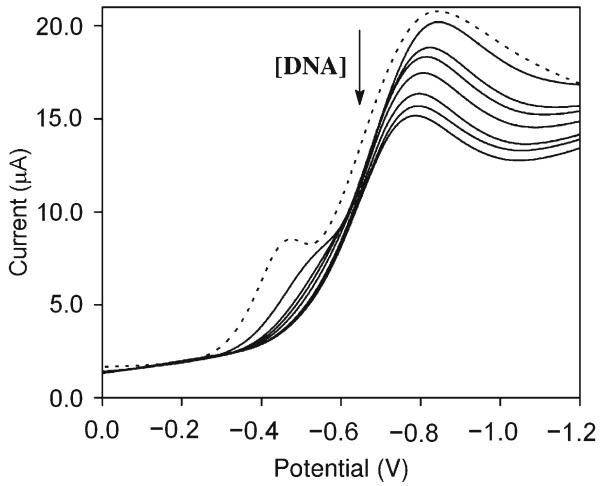


**Fig. 6.** Differential pulse voltammogram of $[CuL]Cl_2$ in the absence (dashed line) and in the presence (solid lines) of different concentrations of DNA.

potential. The resulting changes in the current and potential demonstrate that there is an interaction between Zn(II) and DNA.

Differential pulse voltammogram of the copper complex in the absence and in the presence of varying amount of [DNA] is shown in Fig. 6. An increase in the concentration of DNA causes a negative potential shift along with a significant decrease of the current intensity. The shift in the potential is related to the ratio of the binding constants

$$E_b^{o\prime} - E_f^{o\prime} = 0.0591 \log(K_+/K_{2+}) \quad (5)$$

where $E_b^{o\prime}$ and $E_f^{o\prime}$ are formal potentials of the Co(III)/Co(II) or Ni(II)/Ni(I) or Cu(II)/Cu(I) or Zn(II)/Zn(0) complex couples in the bound and in the free form, respectively. The ratio of the binding constants ($K_{[red]}/K_{[oxd]}$) for DNA binding of the synthesized complexes were calculated and found to be less than one. The above electrochemical experimental results indicate preferential stabilization of Co(II), Ni(II), Cu(II), and Zn(II) forms on binding to DNA over other forms.

Differential pulse voltammogram of the presented Zn(II) complex shows a negative potential shift along with a significant decrease of current intensity during the addition of increasing amounts of DNA. This indicates that the zinc ion stabilizes the duplex (GC pairs) by intercalation. Hence, for the complex of the electroactive species (Zn(II)) with DNA, the electrochemical reduction reaction can be divided into two steps

$$[\text{Zn(II)-DNA}] \leftrightarrow \text{Zn(II)} + \text{DNA} \quad (6)$$

$$\text{Zn(II)} + 2e^- \leftrightarrow \text{Zn}^\circ \quad (7)$$

The dissociation constant ($K_d$) of the Zn(II)-DNA complex was obtained using the following equation

$$i_p^2 = \frac{K_d}{[\text{DNA}]}(i_{p^\circ}^2 - i_p^2) + i_{p^\circ}^2 - [\text{DNA}] \quad (8)$$

where $K_d$ is the dissociation constant of the complex Zn(II)-DNA, $i_{p^\circ}^2$ and $i_p^2$ represent the reduction current of Zn(II) in the absence and in the presence of DNA, respectively. Using the above equation, the dissociation constant was determined. The low value of the Zn(II) ion dissociation constant ($5.4 \times 10^{-10}$ mol $L^{-1}$) was indispensable for the replication, degradation and translation of the genetic material of all species.

In addition to the peak potential shift in cyclic voltammetry, the spectral shift in UV absorption titration and the dependence of the ionic strength on the binding constant, viscosity measurements were carried out to provide further information on the nature of the interaction between the complex and DNA. A classical intercalation model demands that the DNA helix lengthens as base pairs are separated to accommodate the bound ligand leading to an increase of the DNA viscosity. In contrast, a partial non-classical intercalation of the ligand could bend (or kink) the DNA helix, reduce its effective length and concomitantly also its viscosity in order to further elucidate the binding mode of the present complex; viscosity measurements were carried out by varying the concentration of the added complex. The effect of the complexes on the viscosity of DNA is shown in Fig. 7.

Relative viscosity of DNA increases with the increase in the concentration of the metal complexes, which is similar to that of the classical intercalators (Wang et al., 2007). The viscosity results unambiguously show that complexes bind with DNA in the intercalation mode. The vanadyl complex predominantly shows surface binding characteristic. This is

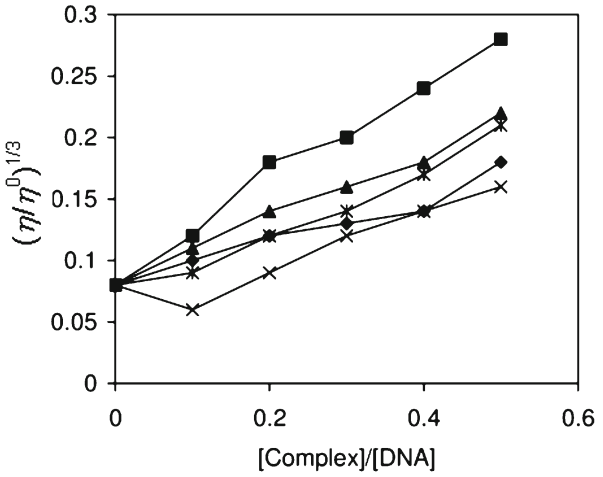


**Fig. 7.** Effect of $[VOL]SO_4$ (∗), $[ZnL]Cl_2$ (×), $[CoLCl_2]$ (♦), $[NiL]Cl_2$ (■), $[CuL]Cl_2$ (▲) on the viscosity of DNA (relative specific viscosity vs. $R$ = [Complex]/[DNA]).

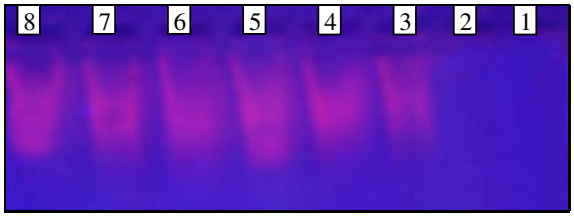


**Fig. 8.** Gel electrophoresis diagram showing the cleavage of SC pUC19 DNA (0.2 μg) by the synthesized complexes (50 μM) in the presence of MPA (5 mM): DNA control (lane 1), DNA + MPA (lane 2), DNA + ligand + MPA (lane 3), DNA + $[CuL]Cl_2$ + MPA (lane 4), DNA + $[VOL]SO_4$ (lane 5), DNA + $[CoLCl_2]$ + MPA (lane 6), DNA + $[ZnL]Cl_2$ + MPA (lane 7), DNA + $[NiL]Cl_2$ + MPA (lane 8).

**Table 5.** Minimum inhibitory concentration of the synthesized compounds against the growth of selected bacteria

| Compound | MIC (mg mL$^{-1}$) | | | |
|---|---|---|---|---|
| | *S. typhi* | *S. aureus* | *B. subtilis* | *E. coli* |
| L | 66 | 58 | 61 | 69 |
| $[CuL]Cl_2$ | 33 | 37 | 33 | 27 |
| $[NiL]Cl_2$ | 35 | 38 | 29 | 22 |
| $[ZnL]Cl_2$ | 39 | 42 | 30 | 31 |
| $[VOL]Cl_2$ | 22 | 19 | 24 | 18 |
| $[CoLCl_2]$ | 34 | 48 | 33 | 28 |
| Streptomycin | 18 | 12 | 10 | 14 |

not surprising since the VO(IV) complex has a square-pyramidal geometry and hence, stacking of the complex between the base pairs is difficult. The other complexes being four coordinate with a planar tetradentate ligand are capable of stacking between the base pairs.

**Table 6.** Minimum inhibitory concentration of the synthesized compounds against the growth of selected fungi

| Compound | MIC (mg mL$^{-1}$) | | | |
|---|---|---|---|---|
| | *A. niger* | *A. flavus* | *C. albicans* | *R. bataicola* |
| L | 77 | 68 | 82 | 79 |
| $[CuL]Cl_2$ | 42 | 31 | 44 | 51 |
| $[NiL]Cl_2$ | 32 | 27 | 39 | 41 |
| $[ZnL]Cl_2$ | 35 | 39 | 32 | 39 |
| $[VOL]Cl_2$ | 22 | 24 | 18 | 27 |
| $[CoLCl_2]$ | 31 | 36 | 42 | 47 |
| Nystatin | 10 | 8 | 12 | 14 |

DNA cleavage of the ligand alone is inactive in the presence of a reducing agent like the 3-mercaptopropionic acid (MPA). The results indicate the importance of the metal in the complex for the observation of the chemical nuclease activity. Oxidative cleavage of pUC19 DNA in the presence of an external reducing agent like MPA (5 mM) was studied by gel electrophoresis using supercoiled (SC) pUC19 DNA (0.2 μg, 33.3 μM) in 50 mM Tris–HCl/50 mM NaCl buffer (14 μL, pH = 7.2) and the complexes (50 μM). From the obtained results, synthesized complexes exhibit significant DNA cleavage activity. Further, the presence of a smear in the gel diagram indicates the presence of radical cleavage (Fig. 8).

With regard to redox chemistry of the synthesized complexes, a plausible mechanism is proposed here. The reaction of M(II)-L (M = Cu(II), Co(II), Ni(II), and Zn(II)) with MPA forms an L-M(I) complex species which abstract C4′-hydrogen atom of the nucleotide adjacent to the 3′-side of guanine. Electrophoretic behavior of the DNA product treated with the L-VO(IV) complex in the presence of MPA suggests a 3′,4′ carbon-carbon scission of the deoxyribose ring initiated by the abstraction of the C4′-hydrogen atom as a trigger reaction. On the other hand, the reaction between the L-VO(IV) complex and MPA may form an active L-V(III) complex species.

For in vitro antimicrobial activity, the investigated compounds were tested against some bacteria and fungi. MIC values of the investigated compounds are summarized in Tables 5 and 6. A comparative study of the ligand and its complexes (MIC values) indicates that the complexes exhibit higher antimicrobial activity than the free ligand. From the MIC values results that compound $[VOL]SO_4$ is more potent than the other investigated complexes and the Schiff base. Such increased activity of the complexes can be explained on the basis of the Overtone's concept (Anjaneyulu & Rao, 1986) and the Tweedy's chelation theory (Dharmaraj et al., 2001). According to the Overtone's concept of cell permeability, the lipid membrane surrounding the cell favors the passage of only

lipid-soluble materials; therefore, liposolubility is an important factor which controls the antimicrobial activity. On chelation, polarity of the metal ion is reduced to a greater extent due to the overlapping of the ligand orbital and partial sharing of the positive charge of the metal ion with donor groups. Moreover, delocalization of the $\pi$-electrons over the whole chelate ring is increased and lipophilicity of the complexes is enhanced. The increased lipophilicity enhances the penetration of the complexes into lipid membranes and blocks the metal binding sites in the enzymes of microorganisms. These complexes also disturb the respiration process of the cell and thus block the synthesis of proteins, which restricts further growth of the organism. Furthermore, the mode of action of the compound may involve formation of a hydrogen bond through the azomethine group with the active centre of cell constituents, resulting in an interference with the normal cell process. In general, metal complexes are more active than ligands as they may serve as a vehicle for activation of ligands as principal cyctotoxic species (Sigel, 1973). Thus, the relationship between chelation and antimicrobial toxicity is very complex and the differences mentioned above are expected to be a function of steric, electronic, and pharmakinetic factors.

## Conclusions

Analytical and spectral data of Ni(II), Cu(II), and Zn(II) complexes suggest a square-planar geometry around the central metal ion. But, Co(II) and VO(IV) complexes have octahedral and square-pyramidal geometry, respectively. Intercalative binding of the Co(II), Cu(II), and Zn(II) complexes with DNA is supported by the electronic absorption spectra, cyclic voltammetry, differential pulse voltammetry, and viscosity studies. In the electrostatic binding mode of the VO(IV) complex with DNA, weak hypochromism and no significant spectral shift were observed in the electronic absorption spectrum. This phenomenon was further confirmed by the viscosity measurements. The synthesized complexes can effectively cleave DNA at a nucleotide adjacent to the 3′-side of guanine such as GC($5' \rightarrow 3'$) and GA($5' \rightarrow 3'$) sequences in the presence of a reductant, MPA. The results obtained from in vitro antifungal and antibacterial tests showed that all the complexes are more active towards bacteria than towards fungi. It has been found that the activities of the complexes are higher than those of the ligand.

*Acknowledgements. The authors gratefully acknowledge the financial support of this work by the Department of Science and Technology, Ministry of Science and Technology, New Delhi, India. They express their heartfelt thanks to the VHNSN College Managing Board for providing the research facilities.*

## References

Angelici, R. J. (1969). *Synthesis and techniques in inorganic chemistry*. Philadelphia, PA, USA: W.B. Saunders Company.

Anjaneyulu, Y., & Rao, R. P. (1986). Preparation, characterization and antimicrobial activity studies on some ternary complexes of Cu(II) with acetylacetone and various salicylic acids. *Synthesis and Reactivity in Inorganic, Metal-Organic, and Nano-Metal Chemistry*, *16*, 257–272. DOI: 10.1080/00945718608057530.

Dharmaraj, N., Viswanathamurthi, P., & Natarajan, K. (2001). Ruthenium(II) complexes containing bidentate Schiff bases and their antifungal activity. *Transition Metal Chemistry*, *26*, 105–109. DOI: 10.1023/A:1007132408648.

Dodwad, S. S., Dhamnaskar, R. S., & Prabhu, P. S. (1989). Electron spin resonance spectral studies of vanadyl complexes with some Schiff bases. *Polyhedron*, *8*, 1748–1750. DOI: 10.1016/S0277-5387(00)80629-4.

Dudley, R. J., & Hathaway, B. J. (1970). Single-crystal electronic and e.s.r. spectra of bis-(aquo)monoaceylacetonatocopper(II) picrate. *Journal of the Chemical Society A: Inorganic, Physical, Theoretical*, *1970*, 1725–1728. DOI: 10.1039/J19700001725.

Firdaus, F., Fatma, K., Azam, M., Khan, S. N., Khan, A. U., & Shakir, M. (2009). Template synthesis and physico-chemical characterisation of 14-membered tetramine macrocyclic complexes, [$MLX_2$] [M = Co(II), Ni(II), Cu(II) and Zn(II)]. DNA binding study on [$CoLCl_2$] complex. *Spectrochimica Acta Part A: Molecular and Biomolecular Spectroscopy*, *72*, 591–596. DOI: 10.1016/j.saa.2008.10.054.

Kannan, N. (1996). *Laboratory manual of general microbiology* (1st ed.). Palani, India: Palani Paramount Publications.

Lever, A. B. P. (1968). *Inorganic electronic spectroscopy* (2nd ed.). New York, NY, USA: Elsevier.

Lu, X., Zhu, K., Zhang, M., Liu, H., & Kang, J. (2002). Voltammetric studies of the interaction of transition-metal complexes with DNA. *Journal of Biochemical Biophysical Methods*, *52*, 189–200. DOI: 10.1016/S0165-022X(02)00074-X.

Marmur, J. (1961). A procedure for the isolation of deoxyribonucleic acid from microorganism. *Journal of Molecular Biology*, *3*, 208–218.

Mitsopoulou, C. A., Dagas, C. E., & Makedonas, C. (2008). Synthesis, characterization, DFT studies and DNA binding of mixed platinum(II) complexes containing quinoxaline and 1,2-dithiolate ligands. *Journal of Inorganic Biochemistry*, *102*, 77–86. DOI: 10.1016/j.jinorgbio.2007.07.002.

Perrin, D. D., Armarego, W. L. F., & Perrin, D. R. (1980). *Purification of laboratory chemicals*. Oxford, UK: Pergamon Press.

Priya, N. P., Arunachalam, S., Manimaran, A., Muthupriya, D., & Jayabalakrishnan, C. (2009). Mononuclear Ru(III) Schiff base complexes: Synthesis, spectral, redox, catalytic and biological activity studies. *Spectrochimica Acta Part A: Molecular and Biomolecular Spectroscopy*, *72*, 670–676. DOI: 10.1016/j.3saa.2008.10.028.

Raman, N., Dhaveethu Raja, J., & Sakthivel, A. (2008). Design, synthesis, spectroscopic characterization, biological screening, and DNA nuclease activity of transition metal complexes derived from a tridentate Schiff base. *Russian Journal of Coordination Chemistry*, *34*, 400–406. DOI: 10.1134/S107032840806002X.

Raman, N., & Jeyamurugan, R. (2009). Synthesis, characterization and DNA interaction of mononuclear copper(II) and zinc(II) complexes having a hard-soft NS donor ligand. *Journal of Coordination Chemistry*, *62*, 2375–2387. DOI: 10.1080/00958970902825195.

Raman, N., Sakthivel, A., & Rajasekaran, K. (2009). Designing, structural elucidation, DNA interaction and antimicro-

bial activities of metal complexes containing tetraazamacrocyclic Schiff bases. *Journal of Coordination Chemistry*, *62*, 1661–1676. DOI: 10.1080/00958970802687554.

Ray, R. K., & Kauffman, G. B. (1990). EPR spectra and covalency of bis(amidinourea/*O*-alkyl-1-amidinourea)copper(II) complexes. Part II. Properties of the $CuN_4^{2-}$ chromophore. *Inorganica Chimica Acta*, *173*, 207–214. DOI: 10.1016/S0020-1693(00)80215-7.

Reichmann, M. E., Rice, S. A., Thomas, C. A., & Doty, P. (1954). A further examination of the molecular weight and size of desoxypentose nucleic acid. *Journal of the American Chemical Society*, *76*, 3047–3053. DOI: 10.1021/ja01640a067.

Satyanarayana, S., Dabrowiak, J. C., & Chaires, J. B. (1993). Tris(phenanthroline)ruthenium(II) enantiomer interactions with DNA: Mode and specificity of binding. *Biochemistry*, *32*, 2573–2584. DOI: 10.1021/bi00061a015.

Sharada, L. N., & Syamal, A. (1992). *Elements of magnetochemistry* (2nd ed.). New Delhi, India: East-West Press.

Sigel, H. (1973). In Sigel, H. (Ed.), *Metal ions in biological systems*. (Vol. *2*: *Mixed-ligand complexes*, pp. 63–125). New York, NY, USA: Marcel Dekker.

Terenzi, A., Barone, G., Silvestri, A., Giuliani, A. M., Ruggirello, A., & Liveri, V. T. (2009). The interaction of native calf thymus DNA with $Fe^{III}$-dipyrido[3,2-*a*:2′,3′-*c*]phenazine. *Journal of Inorganic Biochemistry*, *103*, 1–9. DOI: 10.1016/j.jinorgbio.2008.08.011.

Wang, Q.-X., Jiao, K., Liu, F.-Q., Yuan, X.-L., & Sun, W. (2007). Spectroscopic, viscositic and electrochemical studies of DNA interaction with a novel mixed-ligand complex of nickel(II) that incorporates 1-methylimidazole and thiocyanate groups. *Journal of Biochemical Biophysical Methods*, *70*, 427–433. DOI: 10.1016/j.jbbm.2006.09.011.

Yen, T. F. (1969). *Electron spin resonance of metal chelates* (1st ed.). New York, NY, USA: Plenum Press.